X-Ray Absorption Study of the Ge–Se System

I. GeSe$_2$ Crystalline and Amorphous Phases

C. PEYROUTOU, S. PEYTAVIN, AND M. RIBES

Laboratoire de Physicochimie des Matériaux, USTL, 34060 Montpellier Cedex, France

AND H. DEXPERT

LURE, Bât. 209D, Université Paris-Sud, 91405 Orsay Cedex, France

An EXAFS investigation has been made at both the Ge and the Se K edges to compare the crystalline and amorphous states of the germanium diselenide GeSe$_2$. Special care was taken during sample preparation and it has been possible to analyze the second shell of neighbors which surround germanium. The differences between the specimens are analyzed in terms of a depolymerization factor and related to a clustering process. © 1989 Academic Press, Inc.

Introduction

Chalcogenide glasses are negative photoresists (*1, 2*). After having been sensitized with silver, they can be used to produce VLSI circuits (bilevel inorganic/polymer photoresist structure) since they show an excellent submicrometer resolution (less than 0.5 μm), a high contrast, and a sensitivity over the whole electromagnetic spectrum (deep UV, X-rays, electrons, low-energy ion beams). However, their sensitivity is not great enough and, in order to improve it, a better understanding of the silver photodissolution phenomena is necessary, a point which first requires good knowledge of the structure of these materials. We present here the first steps of our EXAFS study: an investigation on the host matrix, the glassy phase denoted a-GeSe$_2$, and

comparison to the crystallized compound of the same composition, denoted c-GeSe$_2$.

In fact a-GeSe$_2$ has already been the subject of several EXAFS studies, and was one of the first amorphous phases investigated by this technique (*3, 4*). Our results show that great care in the sample preparation for the X-ray absorption measurement is needed for correct structural determination by EXAFS in this particular case. This is due to the lamellar structure of c-GeSe$_2$ used as the reference compound for the backscattered phase and amplitude. This bidimensional organization can be easily disturbed by the mechanical crushing which is commonly used to reduce the powder samples to a suitable grain size for the EXAFS experiments. The present work demonstrates that sample preparation artifacts are the main reason for the absence of

second neighbor signals in the earliest investigations.

I. Sample Preparation and Structural Relationships

The binary Ge–Se phase diagram has two crystalline compounds but only the diselenide which melts at 740°C will be considered here. It is prepared from pure powders of germanium and selenium obtained from Aldrich chemicals (gold label quality). After mixing the stoichiometric quantities, the sample is introduced into a silica capsule, formerly outgassed, and sealed under a good vacuum (10^{-6} Torr). A progressive heating procedure to 980°C at the speed of 6°C per hr, followed by a continuous double-axis rotation of the furnace during 12 hr gives good homogeneity to the melted medium. The crystal germination is obtained through a very slow cooling process within the closed furnace to avoid any oxygen contamination. The final product is in the shape of soft, orange-yellow-colored, thin platelets.

From the curve published by Azoulay *et al.* (5) the preceding thermal cycle must be terminated by a rapid temperature quenching in a solution of salted water maintained at less than 0°C to prepare the amorphous phase. These operating conditions lead to some cracks of the final glass even after reannealing the specimen at 280°C, a temperature slightly less than the Tg (glass transition temperature). The local chemical composition is monitored by energy dispersive X-ray analysis using a scanning electron microscope.

The high-temperature form $GeSe_2\alpha$, c-$GeSe_2$ crystallinized in the monoclinic system with the space group $P2_1/c$. It is a lamellar structure with each of the lamellar entities made of a series of parallel linear chains formed by $[GeSe_4]_{1/2}$ tetrahedra-sharing vertices. They are bound together by bridges of two tetrahedra sharing one

edge (6). Thus each germanium atom is tetracoordinated while the selenium atoms are surrounded by two germaniums. The links between two of these layers come from van der Waals bonds; the homopolar Ge–Ge or Se–Se associations do not exist in this crystal form.

Figure 1 details the basic unit of that structure. It shows that the local environment of a germanium atom, at a distance less than 4 Å, consists of:

—four selenium atoms forming the tetrahedron of the first coordination shell at a mean distance of 2.352 Å;

—two other types of germanium atoms located on two different sites. One, at 3.049 Å, is in between two germaniums which are at the center of tetrahedra linked by their edges. The other type belongs to the tetrahedra joined by one vertex, and, as this atom is shared between several of these polyhedra, it counts per 3.33 atoms at a distance of 3.559 Å from the central germanium taken as origin.

As it has been shown by Raman spectroscopy (7), the local order in a-$GeSe_2$ is very similar to that existing in c-$GeSe_2$. It is not the same at medium range distance and thus some difference should be seen at low k in the $\chi(k)$ absorption signal. However,
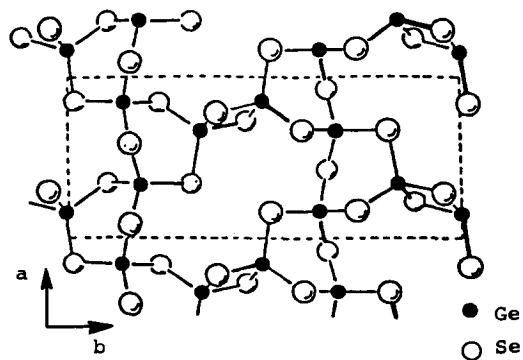

FIG. 1. The basic unit of c-$GeSe_2$ projected along the [001] axis.

the curves given in the literature (3, 4) do not present any significant changes between the crystal and the glass. The question is then to determine the reason for that similarity. One possible reason is disorganization of the stacking sequence of the lamellar structure of c-GeSe$_2$ caused by the sample crushing usually done before data collection. We therefore undertook a systematic study of this effect in order to define a preparation procedure which does not affect the crystallinity. Before considering the EXAFS spectra, we have used three other probes to monitor the effects of different sample preparation procedures.

In the first, X-ray diffraction was used to follow the progressive disappearance of crystallinity with three different types of crushing:

(1) hand grinding for a few minutes results in a slight diminishment of the heights of the diffraction peaks;

(2) long mechanical grinding over several hours almost fully erases these peaks and transforms them into diffuse rings characteristic of a poorly organized state;

(3) and finally a low-temperature grinding in liquid nitrogen to minimize the energy transport, in which case, the diffraction pattern of the fine powder produced is made of intense and well-resolved peaks very similar to those given by the starting c-GeSe$_2$.

The second probe we used is Raman spectroscopy. Figure 2 gives the Raman spectra corresponding to the three kinds of crushing and the one of a-GeSe$_2$ in the energy range characteristic of the A$_1$ and A$_1^c$ bands. Our GeSe$_2$ crystal and glass spectra ((1) and (4), respectively) are the same as those published in the literature (8). The main feature is the existence of the so-called "companium line," A$_1^c$, in the vitreous phase. This band is clearly visible on spectrum (3) too, a spectrum obtained from
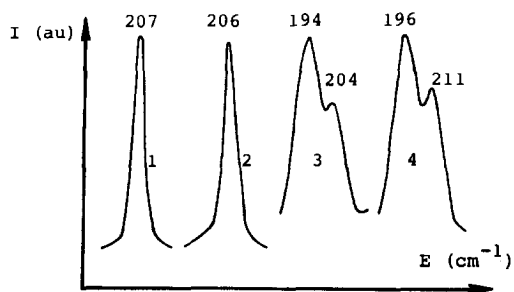

FIG. 2. Raman spectra of the different samples in the energy range of the A$_1$ and A$_1^c$ bands. (1) c-GeSe$_2$ used as reference. (2) c-GeSe$_2$ after hand grinding. (3) c-GeSe$_2$ after long mechanical grinding. (4) a-GeSe$_2$ synthesized by classical quenching.

the mechanically crushed c-GeSe$_2$. We must point out the similarity of the Raman signals of the two glassy materials, one classically prepared by temperature quenching, the second by crushing the crystal.

The last parameter we examined to check the amorphization process is the temperature of vitreous transition, Tg, and differential calorimetry has been used to do so. The thermogram obtained from the mechanically crushed powder has an endothermic break around 350°C, the shape of which is that of a vitreous transition. This value is moreover very close to the Tg value of a-GeSe$_2$ obtained by temperature quenching, 362°C.

There is therefore no doubt that one must pay attention to the sample preparation technique for X-ray absorption measurements before drawing any conclusions as to the existence (or not) of medium-range order in these materials. The number of contributions appearing in the radial distribution function of the EXAFS signal will be strongly dependent on the preparation mode. Consequently this raises questions about the a-GeSe$_2$ and c-GeSe$_2$ spectra given in the literature where such details are not reported.
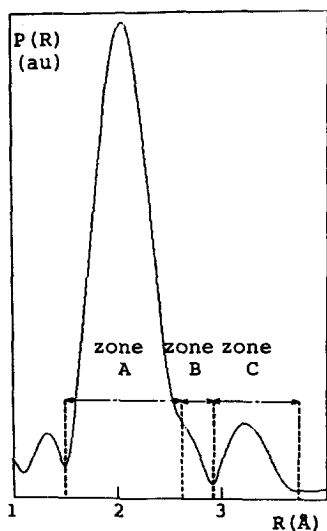
FIG. 3. The Fourier transform modulus uncorrected for phase shift of c-GeSe₂ at the germanium K edge. A, B, and C are the three zones considered in the analytical procedure.

II. EXAFS Investigation

The experiments have been carried out at LURE DCI operating at 1.72 GeV with a 200 mA current. Ge and Se K edges (11104 and 12658 eV, respectively) have been measured at room temperature, using either a Si (220) channel-cut, or a Si (311) double crystal monochromator. The analytical procedure has been fully described elsewhere (9); the normalized oscillatory part of the absorption spectra is k^3-weighted and Fourier transformed through a Haning window. The atomic parameters (amplitude and phase shifts) are extracted from spectra recorded under the same conditions from the crystalline compound. Fits of the experimental signals use a mean least-squares refinement involving a maximum of two shells at the same time.

II. A. Germanium K Edge

The Fourier transform modulus of c-GeSe₂ uncorrected for phase shift at the germanium edge is reported in Fig. 3. It

presents three features between 1.5 and 4 Å:

—a main contribution which peaks at 2.05 Å (zone A);

—a side lobe on the right part of that first contribution, of weak intensity (zone B);

—another well-defined contribution at 3.2 Å (zone C) corresponding to the Ge–Ge distance which separates successive tetrahedra linked by their summits.

These measured values are less than the crystallographic data by 0.2 to 0.3 Å, a difference coming from the phase shifts which are taken into account when fitting the signals.

Questions must be asked about the significance of the second feature, visible on the right side of the germanium–selenium pair. As a matter of fact, it could correspond to the Ge–Ge distance between two tetrahedra sharing one edge and, thus, be of great importance to the complete description of the crystal disorganization into the amorphous phase. One contradiction with this assignment appears immediately when the selenium edge (Fig. 4) is considered. The side lobe of zone B still exists although the structure has no selenium neighbor at this distance. That forces us to analyze in full detail this germanium side lobe, taking in
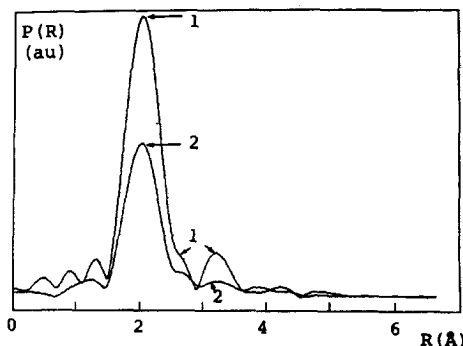

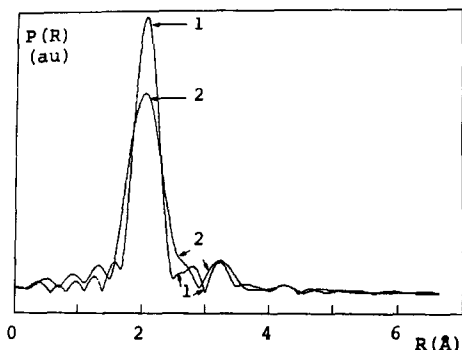FIG. 4. Comparison of the Fourier transform moduli of c-GeSe₂ at the Ge K (spectrum 1) and Se K (spectrum 2) edges.

FIG. 5. Fourier transform moduli of c-$GeSe_2$ at the Ge K edge. Spectrum 1 is obtained with the large Haning window (14 Å^{-1}), spectrum 2 with the small one (10 Å^{-1}).
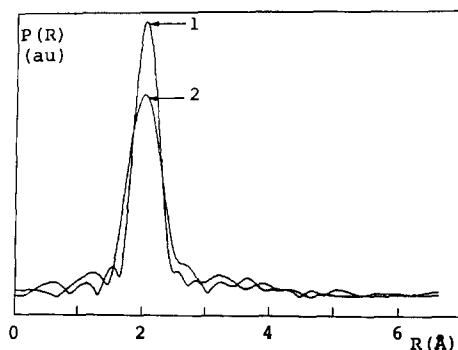

FIG. 6. Fourier transform moduli of c-$GeSe_2$ at the Se K edge. Spectrum 1 corresponds to the large energy window, spectrum 2 to the small one.

account two energy windows for Fourier transforming the experimental data (one stretches over 10 Å^{-1}, the second over 14 Å^{-1}) to determine:

if this shoulder really comes from the atomic arrangement;

what the energy limits are for the best analytical procedure.

Figures 5 and 6 are the radial distribution functions at the germanium and selenium edges, respectively, calculated with the two energy bandwidths. In both cases, when the large window is used, the side lobe changes to a new shape made of complex ripples. They are well separated from the main Ge–Se first peak, but without any structural correlations.

That side lobe is also seen in pure germanium (Fig. 7) still without any atomic position significance. It is once again clearly visible in data published on the subject (3, 4) or from other nearby elements of the periodic table such as arsenic (10).

We consequently will not consider this feature as related to the atomic arrangement but as depending solely on the analytical conditions. A point in line with this assumption comes from observations one can make on the shape and position of the cor-

responding experimental backscattering amplitudes. Teo and Lee (9) have shown some years ago that the maximum P of a backscattered amplitude is related to the atomic number of one atom Z by the linear relationship $P = 0.204\ (Z + 8)$. Even for our situation where we extract these parameters from experimental signals, which means that the corresponding amplitudes include the central atom phase shifts, we find that the P values are much more reasonable when using the 10-Å^{-1} Haning window. In that case, the differences in peak position remain below 1.5 Å^{-1} instead of 2.5
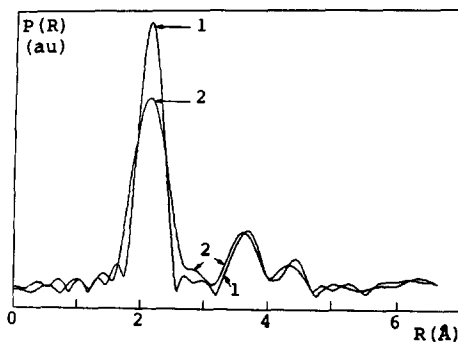

FIG. 7. Fourier transform moduli of pure germanium coming from the large (spectrum 1) and small (spectrum 2) energy range.

Å^{-1} with the 14-Å^{-1} energy window. Therefore we have chosen this 10-Å^{-1} energy range for all our investigations.

Two series of simulations have been undertaken to fit the first germanium environment. As in c-GeSe$_2$ the Ge–Se distances vary from 2.337 to 2.369 Å; we tried (i) a one-shell model which gives the average situation and (ii) a two-subshell adjustment, hoping to get an image closer to the real deformed GeSe$_4$ tetrahedron which exists in the crystal phase. In fact, the improvement of the resulting reliability factor was not great enough to be significant, remaining within the accuracy limits, so that we decided to consider only a one-shell fitting procedure.

If the first coordination sphere remains almost unchanged from c- to a-GeSe$_2$, the second neighbor's contribution is noticeably modified in the glassy phase as half of the Ge–Ge pairs have been ruptured. This second shell, which has been ignored in the previous studies published in the literature, is a direct indication of the depolymerization of the tetrahedron chains. It can be used as a fingerprint of the formation of the crystallized domain within the amorphous phase. In the reference compound c-GeSe$_2$, an infinite layer is not, of course, depolymerized and each germanium has 3.33 neighbors at 3.56 Å average. If N is the corresponding neighbor number for a-GeSe$_2$, we define the percentage of depolymerization by:

$$D = \left(\frac{3.33 - N}{3.33}\right) \times 100.$$

A key point is the evaluation of the coordination number and Debye–Waller (disorder order, thermal motion) correlation effects. To be sure that the signal is only affected by the variations of N, we fixed it once at the value of 3.33 (R is at 3.55) and looked at the a-GeSe$_2$ $\chi(k)$ adjustment. The Debye–Waller difference with the crystal then increases to 0.2 Å, an unacceptable value for a solid.

We also considered the log $[\chi(c\text{-GeSe}_2)]/[\chi(a\text{-GeSe}_2)]$ function and plotted it versus k^2 (Å^{-2}). The result we obtained is shown in Fig. 8 and is in very good agreement with the data obtained from the simulation (see Table I). This indicates definitely that the loss of amplitude of this second contribution is a result of a decrease in the neighbor number and not of a change in the Debye–Waller value stemming from a larger dispersion of the Ge–Ge distances. The depolymerization factor D we defined above is thus fully realistic and could be related to the outrigger raft model discussed by Phillips et $al.$ (11). Its calculation from the EXAFS fits of the other GeSe$_2$ or GeSe$_x$ vitreous phases will be a good guide for describing the amorphization process.

II. B. Selenium K Edge

As the selenium–selenium pairs are largely scattered in c-GeSe$_2$, the first shell formed by the two germanium atoms at 2.352 Å has only been investigated in the glassy compositions. A one-shell model is also used there solely, as the fits we tried with two subshells, in the same way as those tried in the case of germanium, lead
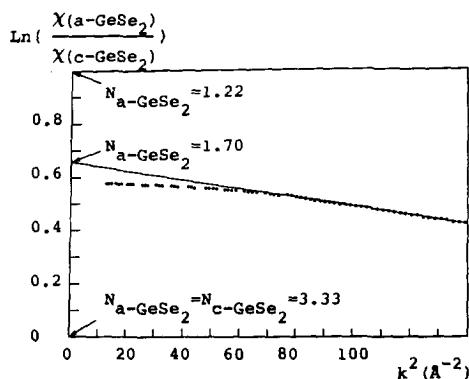
FIG. 8. Plot of ln[$\chi(c$-GeSe$_2$)]/[$\chi(a$-GeSe$_2$)] function of k^2.

TABLE I

Fit Results at the Germanium Edge for the First and Second Coordination Spheres

	First coordination sphere: Ge–Se bonds[a,b]					Second coordination sphere: long Ge–Ge distances[a,c]					
	N	R(Å)	$\Delta\sigma$(Å)	ΔE(eV)	RF(10^{-3})	N	R(Å)	$\Delta\sigma$(Å)	ΔE(eV)	RF(10^{-3})	$D\%$
c-GeSe$_2$ material [2]	3.99	2.35(6)	0.012	1.19	0.06	2.99	3.55(7)	0.003	0.29	0.19	10.2
c-GeSe$_2$ material [3]	3.80	2.35(5)	0.005	0.77	0.11	1.85	3.55(9)	0.019	2.82	2.77	44.5
a-GeSe$_2$ material [4]	3.87	2.35(7)	0.018	2.30	0.11	1.81 1.7*	3.55(2)	0.020 0.028*	1.97	1.81	45.8

Note. RF and D are the reliability and depolymerization factors, respectively. * indicates the N and $\Delta\sigma$ measured values from Fig. 8.
[a] Material [1] was used as reference.
[b] $N = 4$, $R = 2.352$ Å.
[c] $N = 3.33$, $R = 3.559$ Å, $D = 0\%$.

practically to the same reliability factors as those obtained with the one-shell model.

III. Discussion and Conclusion

The structural studies have been made therefore on four materials:

(1) c-GeSe$_2$ crushed at low temperature and used as a reference;

(2) partially crystallized GeSe$_2$ obtained from hand crushing;

(3) vitreous GeSe$_2$ prepared from long mechanical crushing;

(4) vitreous GeSe$_2$ synthesized by classical quenching.

At the germanium edge, the radial distribution function shows effectively the influence of the sample preparation (Fig. 9). When the energy transfer increases during the powder crushing, the degree of disorder is enhanced as one can qualitatively follow from spectra (1) to (2) and (3) toward the signal of the completely vitreous phase obtained from quenching (4). Table I lists the fit results for the first and second shells surrounding the germanium atoms.

For the first coordination sphere, the decrease in the amplitude is within the error limits but probably corresponds to the introduction of statistical disorder; the Ge–Se distances should be a little bit more stretched within the tetrahedron. The second coordination sphere is more sensitive to the powder preparation which breaks the selenium bridge and gives rise to depolymerization of the chains.

As indicated in Table I a strong similarity exists between the two vitreous compounds (3) and (4). They have the same degree of depolymerization and an identical averaged Ge–Ge distance, 3.55 Å.
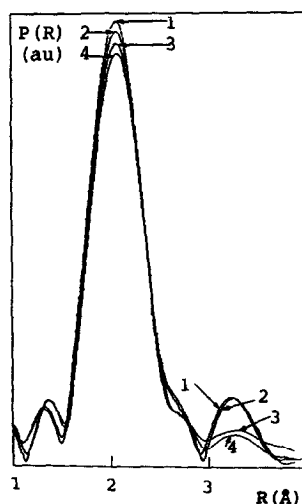
At the selenium edge, once again, the

FIG. 9. Radial distribution functions uncorrected for phase shift at the Ge K edge of the four different materials considered in this study.
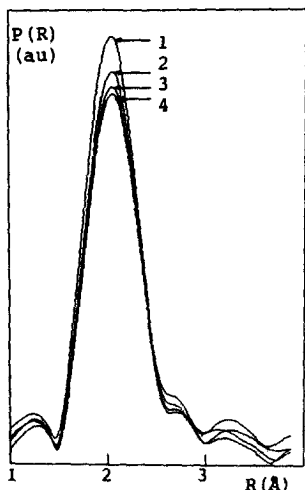
FIG. 10. Same radial distribution functions as those in Fig. 9 but at the Se K edge.

TABLE II

FIT RESULTS AT THE SELENIUM EDGE

	First coordination sphere: Se–Ge bonds[a]				
	N	$R(\text{Å})$	$\Delta\sigma(\text{Å})$	$\Delta E(\text{eV})$	$RF(10^{-5})$
c-GeSe$_2$ material [2]	1.79	2.35(4)	0.019	1.63	0.35
c-GeSe$_2$ material [3]	1.89	2.35(8)	0.012	0.80	0.78
a-GeSe$_2$ material [4]	1.87	2.35(9)	0.019	1.27	0.11

[a] Material [1] was used as reference. $N = 2$, $Re = 2.352$ Å.

first shell amplitude is affected by the preparation method (Fig. 10), even more than in the case of germanium. The Ge–Se distances appear to increase very slowly as a function of disorder, this change remaining however, within the inaccuracy of the calculation (Table II): from 2.35(2) Å in (1) to 2.35(4) (2), 2.35(8) (3) and 2.35(9) in (4).

The main point of the present work is therefore the clear evidence that careful sample preparation is critical for X-ray absorption measurements, especially when layered phases are compared with their amorphous related compositions. Various probes (X-ray diffraction, Raman spectroscopy, etc.) can define the successive steps of the phase transformation but the EXAFS investigation allows quantification of the depolymerization process through the study of the second neighbor changes. This new point, never seen before, even for these GeSe$_2$ compounds, demonstrates a loss of almost half of the second germanium–germanium pairs. This is in line with a clustering process as it is highly probable that the selenium atoms displaced when the Ge–Se bonds are broken may easily recom-

bine to form homoatomic pairs, as the outrigger raft hypothesis underlines (11). Last but not least, this work gives us a good experimental basis for the study we have made of the GeSe$_x$ phases enriched in selenium, investigation of which is discussed in the second part of this work.

References

1. P. G. HUGGETT, K. FRICK, AND H. W. LEHMANN, *Appl. Phys. Lett.* **42**, 592 (1983).
2. W. LEUNG, N. W. CHEUNG, AND A. R. NEMEUTHER, *Appl. Phys. Lett.* **46**, 481 (1985).
3. D. E. SAYERS, E. A. STERN, AND F. W. LYTLE, *Trans. Amer. Crystallogr. Assoc.* **10**, 45 (1974).
4. D. E. SAYERS, F. W. LYTLE, AND E. A. STERN, in "Amorphous and Liquid Semiconductors" (J. Stuke and W. Brenig, Eds.), p. 203 (1974).
5. R. AZOULAY, H. THIBIERGE, AND A. BRENAC *J. Non-Cryst. Solids* **18**, 33 (1975).
6. VON G. DITTMAR AND H. SCHAFER, *Acta Crystallog. B* **32**, 2726 (1983).
7. J. A. ARONOVITZ, J. R. BANAVAR, M. A. MARCUS, AND J. C. PHILLIPS, *Phys. Rev. B* **28**, 4454 (1983).
8. P. M. BRIDENBAUGH, G. P. ESPINOSA, J. E. GRIFFITHS, J. C. PHILLIPS, AND J. P. RENEIKA, *Phys. Rev. B* **20**, 4140 (1979).
9. B. K. TEO AND P. A. LEE, *J. Amer. Chem. Soc.* **101**, 2815 (1979).
10. A. M. FLANK, D. BAZIN, H. DEXPERT, P. LAGARDE, C. HERVO, AND J. Y. BARRAUD, *J. Non-Cryst. Solids* **91**, 306 (1987).
11. J. E. GRIFFITHS, J. C. PHILLIPS, G. P. ESPINOSA, J. P. RENEIKA, AND P. M. BRIDENBAUGH, *Phys. Status Solidi* **122**, K11 (1984).